INSTITUTE OF PLASMA PHYSICS

NAGOYA UNIVERSITY

RESEARCH REPORT

NAGOYA, JAPAN

Radio-Frequency Plugging of a High Density Plasma

T. Watari, T. Hatori, R. Kumazawa, S. Hidekuma,
T. Aoki, T. Kawamoto, M. Inutake, S. Hiroe,
A. Nishizawa, K. Adati, T. Sato, T. Watanabe,
H. Obayashi, K. Takayama

IPPJ- 331

APRIL 1978

Further communication about this report is to be sent to the Research Information Center, Institute of Plasma Physics, Nagoya University, Nagoya, Japan.

Abstract

Mirror end loss can be suppressed by applying an rf field at the mirror throat through low impedance coils. This method is verified to be effective for a high density plasma up to 10^{14} cm^{-3}. Experimental results shows that the rf field strength required for the plugging is differently dependent on the plasma density according to the type of coil. The mechanism of giving the density dependence is theoretically clarified for each coil. Particularly, it is shown that the electric field induced in the direction of the static magnetic field is intrinsic for the density independent result of type 3 coil.

1. INTRODUCTION

When an rf field is applied to a charged particle in a magnetic field, it feels a quasi-potential$^{1)}$

$$\phi = \frac{q^2E^2}{4m} \frac{1}{\omega^2 - \omega_c^2} , \tag{1}$$

where q, m, ω_c, ω, and E denote the charge, the mass the local cyclotron frequency, the frequency of applied rf field and its intensity. Such potential can be used to reduce plasma loss from an open-ended system. In so far, our works have been concentrated on the plugging of a line cusp end.$^{2-5)}$ In a line cusp, the plasma forms a thin sheet whose thickness is of the order of the local ion Larmor radius. We have adopted a parallel plate rf electrodes sandwiching such a sheet plasma. It has been shown experimentally that the rf voltage needed for plugging is proportional to plasma density$^{3)}$ or to square root of it,$^{5)}$ in the density range lower than 10^{12} cm^{-3}. In these experiments we have found the most effective plugging condition is achieved at a certain frequency somewhat higher than the local ion cyclotron frequency. It has been shown that an electrostatic ion cyclotron mode plays an important role in the plugging experiment in the low density regime.

In the high density regime, on the contrary, an electromagnetic ion cyclotron mode is expected to be important. We intend to study rf plugging of the high density plasma in this paper. To excite the electromagnetic mode we prepare some kinds of low impedance rf coils, instead of parallel plate electrodes. In this experiment, we use a simple magnetic mirror geometry. The experimental results are discussed and compared with a simplified slab model theory by which the rf plugging mechanism is dealt systematically with for various kinds of coupling schemes.

II. EXPERIMENT

The experiment is carried out on TPD-III machine shown in Fig.1. It is a linear machine consisting of four sections: plasma source, differential pumping section, experimental region and burial chamber. TPD-type plasma source is used in the experiment with working gas H_2 or He. It is operated in quasi-steady mode of 30 ms duration and 5 s interval. The discharge current is about 200 A. The plasma flows out through the anode hole and is lead to the differential pumping sections, where neutral particles are scraped away. The burial chamber is used also to assure the high degree of ionization in the experimental region. The pressure of the neutral particle in the experimental region is kept less than 1×10^{-5} torr, under which rf discharge is negligible. The plasma density is up to 10^{13} cm^{-3} in the experimental region. The diameter of the plasma column is about 2 cm. Electron and ion temperatures range from 10 to 20 eV. To get a plasma in the density range from 10^{13} to 10^{14} cm^{-3}, we used an MPD plasma source.6) It is operated with a fast acting valve to keep the high degree of ionization. The discharge current is about 10 kA and plasma duration is about 1 ms. The plasmas produced by these two kinds of plasma sources are quite similar, excepting their density range. A mirror magnetic field is produced in the experimental region by exciting B-coil shown in Fig.1. The axial distribution of the magnetic field intensity is shown in Fig.2. Since we are studying the density dependence of rf plugging, the most important quantities are the plasma density in the center of the mirror and the plasma loss flux from the mirror throat. We deduce the density from the data of double probe, 70 GHz and 24 GHz microwave interferometers, and diamagnetic loop. The double probe is movable in a radial direction and it offers density profile. The plasma density given by these methods agrees with each other in factor 2. The density used in the following description of experimental data is that obtained by double probe. The loss flux is measured by a multi-grid energy analyzer and a plane probe. The former is large enough to collect all the loss flux, while the latter is movable in radial direction giving profile of loss flux. The loss flux which appears in the following description of experiment is that measured by the multi-grid analyzer. We improved this by furnishing with 20 μm slits on the front mesh for a high density plasma. Ion and electron temperatures are measured with this analyzer. Electron temperature is also measured by the double probe at the center of the mirror.

We designed three types of rf coils which are shown in Fig.3. Type 1 is an ordinary 7-turn solenoid, type 2 is a pair of half turn coils, and type 3 is similar to the one used by Ovchinnikov et al.$^{7)}$ in the heating of a stellarator plasma. They are alternative set up in the mirror throat and tested. Since they are made in the same size (6 cm in diameter and 10 cm in length), experimental data of these coils can be directly compared. The rf field (6.26 MHz) is supplied from 100 kW rf oscillator through 50 Ω rf feeder. The ω/ω_c value computed with the local cyclotron frequency at the center of the coil is 0.82, and the point where $\omega/\omega_c = 1$ locates inside the coil (see Fig.2).

Figure 4a is a typical signal of multi-grid analyzer when TPD source is used. A remarkable decrease of loss flux is observed during 1 ms when rf field is applied. Figure 4b shows ion loss flux with and without rf field when MPD source is used. Here, we used a 500 kW rf oscillator with lower feeding impedance (12 Ω) to reduce the reaction from the plasma. To prove that such remarkable decrease of loss flux is not due to the decrease of the plasma density in the center of the mirror, we measured it with the movable double probe. Though radial distribution of the plasma density becomes somewhat broader with rf field, the density integrated over the plasma radius does not decrease. Similarly, to verify that the decrease of the loss flux is not due to the broadening of loss flux beyond the aperture of the multi-grid analyzer, we measured the profile of loss flux with the movable plane probe. The loss flux integrated over the plasma radius agrees with that measured by the multi-grid analyzer. The electron density measured behind the rf coil by microwave interferometer also decreases with rf field. It implies that electrons are also plugged to establish charge neutrality. We define relative loss flux as the loss flux divided by that without rf field. Therefore, $\alpha = 0$ indicates perfect rf plugging. Figure 5 shows experimentally obtained dependence of α on the rf voltage when type 3 coil is used. It is observed in Fig.5 that α is a decreasing function of rf voltage V_{rf} and increasing function of plasma density n. Similar tendencies are obtained for other two coils. Figure 5 offers also the information how high rf voltage is required for various value of the plasma density to achieve 90% reduction ($\alpha = 0.1$) of loss flux. Such relations are obtained for three coils and compared in Fig.6. We assume an empirical relation of the form $\alpha = \exp[-A(V_{rf}/n^{x})^{y}]$ and determine A, x and y from Figs.5 and 6. We obtain

$$\alpha = \exp[-0.44(V_{rf}/n^{0.1})^{1.8}], \quad \text{for type 3.} \tag{2}$$

Similarly,

$$\alpha = \exp[-0.08(V_{rf}/n)^{1.8}], \quad \text{for type 1} \tag{3}$$

and

$$\alpha = \exp[-1.10(V_{rf}/n^{0.6})^{1.8}, \quad \text{for type 2.} \tag{4}$$

Here, V_{rf} is measured in [kV] and n is measured in [10^{12} cm^{-3}]. The fact that plugging with type 3 coil depends slightly on plasma density is particularly important if we consider the application to the thermonuclear fusion. Therefore we conclude that type 3 coil is the most favourable geometry among these three coils.

It has been reported in previous works[2,3] that the rf frequency which gives the maximum plugging is about 1.5 times higher than ion cyclotron frequency. However, since present work differs from former one in rf launching method and plasma density regime, the frequency dependence may appear differently. We measured it for type 3 coil. Since the rf coil has very low impedance, we designed low impedance feeder to take out the matching circuit from the vacuum chamber. The frequency sweep is thereby made possible. Furthermore, we made the mirror ratio small by exciting E coils as well as B coils. Otherwise a wide variation of magnetic field intensity inside the rf coil makes the frequency dependence obscure. The profile of the magnetic field is shown in Fig.2 by a broken line. Figure 7 shows the experimentally obtained frequency dependence of α value. The optimum frequency is plotted in Fig.8 against the rf voltage. The extrapolation of the curve toward weak rf field falls in a frequency lower than the ion cyclotron frequency. Many works[8] have been done in the linear theory concerning to the transverse ion cyclotron wave in the frequency range lower than the ion-cyclotron frequency. We suppose that when an rf frequency coincides with an eigenfrequency of the transverse wave, a good penetration of the rf field occurs with resonant decrease of loss flux. It corresponds to the fact that rf plugging is effective in the low density plasma due to the excitation of electrostatic eigenmode.

III. THEORY

For simplicity we consider a slab geometry which is shown in Fig.9. It is not difficult to extend our analysis to a cylindrical geometry. The plasma is assumed to be homogeneous in the y-direction and to have a thickness 2λ in the x-direction. The static magnetic field is set in the z-direction. A pair of electrodes of length ℓ in the z-direction are located at x = ± d. The case a) represents a model for the rf plugging of a sheet plasma by the plane parallel electrodes, on which an rf voltage V_{rf} is applied. When we give a sheet current I_0, the cases b) and c) correspond to type 2 and type 3 coils, respectively. The difference between type 2 and type 3 is the direction of the current. The vacuum electromagnetic field is shown in Fig.9.

Since the data in Fig.6 are obtained under the condition of fixed ω, Eq.(1) indicates the square of the rf field intensity determines the plugging efficiency. Therefore, penetration of the rf field is essential for the rf plugging. We use the cold approximation for ions and the drift approximation for electrons. The cases a) and c) can be treated simultaneously, and the expressions for the rf field at x = 0 are given by

$$E_x = \left(E_x^0 + k_D^2\lambda^2 \frac{\frac{\omega}{ck_z} B_y^0}{1 - \frac{\omega^2}{c^2k_z^2} k_D^2\lambda^2}\right)/\varepsilon(\lambda^2), \qquad (5)$$

$$E_y = \frac{i\omega}{\omega_c} \frac{\omega_p^2\lambda^2}{c^2} \frac{\omega^2}{\omega^2-\omega_c^2 + \frac{\omega_p^2\lambda^2}{c^2}\omega 2} E_x, \qquad (6)$$

$$\frac{\partial}{\partial x} E_z = (ik_z E_x - \frac{i\omega}{c} B_y^0)/(1 - \frac{\omega^2}{c^2 k_z^2} k_D^2 \lambda^2), \tag{7}$$

where the dielectric constant ε is defined by

$$\varepsilon(\lambda^2) = 1 - \frac{\omega_p^2}{\omega^2 - \omega_c^2} + \frac{k_D^2 \lambda^2}{1 - \frac{\omega^2}{c^2 k_z^2} k_D^2 \lambda^2} (1 - \frac{c_s^2 k_z^2}{\omega^2}). \tag{8}$$

Here k_D, ω_p, ω_c are electron Debye wave number, ion plasma frequency, and ion cyclotron frequency, respectively. The parallel wave number k_z is estimated to be π/ℓ. In deriving in Eqs.(5) - (7) we have also assumed the following conditions satisfied by the present experiment: $c_s^2/c_A^2 << 1$, $c_s^2/\lambda^2\omega_c^2 << 1$, $k_z^2\lambda^2 << 1$, $\omega_p^2\lambda^2/c^2 << 1$, and $k_D^2\lambda^2 >> 1$, where c_s and c_A are the ion sound and the Alfven velocities. The quantity E_x^0 in Eq.(5) is the vacuum field given by V_{rf}/d for parallel plate electrodes, and B_y^0 represents the vacuum rf magnetic field for type 3 coil. For the case of parallel plate electrodes, the field is screened inversely proportional to the density. On the other hand, the second term in the numerator of Eq.(5) is proportional to the density and cancels the density dependence in the dinominator. Therefore, we get the rf field in the plasma independent of density for type 3 coil. It is just the explanation for the present experimental result.

The essential point for the mechanism of efficient rf plugging by type 3 coil is the existence of E_z, the component of the rf electric field parallel to the static magnetic field, as illustrated in Fig.10. The electrons respond quickly to the E_z and obey the Boltzmann distribution, $n_e = n_0 e\ /T_e$, where ψ is the parallel potential, defined by $E_z = -(\partial/\partial Z)\psi$. The function $\psi(x, z)$ is an odd function of x for the present situation, so that the induced electron charge density $-en_e$ causes electrostatically an rf electric field E_x in the x-direction. Thus the driving source of E_x is proportional to the plasma density, if the magnetic screening by the plasma is negligibly small. Therefore, E_x in the plasma is independent of the density, although it is screened by the dielectric constant ε proportional to the density. This is the reason why the rf plugging efficiency is independent of the density for type 3 coil. The current I_z carried by electrons flow parallel to the static magnetic field in such a way to satisfy the continuity equation for electrons. The perpendicular current I_x is carried by ions driven by E_x. It should be remarkable that the induced loop current flows in the plasma paramagnetically to the external coil current. The perpendicular rf magnetic field B_y at x = 0 is found to be $B_y(0) = B_y^o/[1 - \frac{2}{c^2k_z^2}\frac{\omega_p^2}{\frac{c_s^2}{\lambda^2} - \omega^2 + \omega_c^2}]$. We can see that the rf magnetic field in the plasma is enhanced for the relatively low density plasma in the case $\omega < \omega_c$. When the plasma density increases further, $B_y(0)$ will change its direction at the singular point, where the frequency coincides with the eigenfrequency of the electromagnetic ion cyclotron wave. If the plasma density is higher than this singular density,

$B_y(0)$ will be screened diamagnetically. Therefore, in the case, $\omega_p^2 > (c^2k_z^2/\omega^2)(\omega_c^2 - \omega^2 + c_s^2/\lambda^2)$, the effectiveness of type 3 coil may be limited.

Equation (5) offers the information about eigenfrequency of plasma under the present situation. A numerical solution for equation, $\varepsilon = 0$, is shown in Fig.10. The experimental condition of Fig.6 is indicated by an arrow in Fig.10. The optimum frequency is then somewhat lower than ion cyclotron frequency, demonstrating the agreement with the experimental result obtained by extrapolation in Fig.8. The disagreement in the high rf field intensity regime may come from the nonlinear effect.

Similarly we obtain the expression for the field at the midplane, for type 1 and type 2 coils

$$\frac{\partial}{\partial x} E_x = \frac{-\dfrac{\omega^2}{\omega_c c} B_z^0}{\dfrac{\omega^2-\omega_c^2}{\omega_p^2} + \dfrac{\omega^2\lambda^2}{c^2}(1 - \dfrac{\omega_p^2}{c^2k_z^2}\dfrac{\omega 2}{\omega_c^2}} \frac{1}{\varepsilon'} \tag{9}$$

$$\frac{\partial}{\partial x} E_y = \frac{\omega^2 - \omega_c^2}{\omega_p^2} \frac{\omega_c}{i\omega} \varepsilon \left(\frac{\lambda^2}{2}\right) \frac{\partial E_x}{\partial x}, \tag{10}$$

$$E_z = -ik_z \frac{1}{k_D^2} \left[\frac{\omega_p^2}{\omega^2-\omega_c^2} + \frac{\omega_c^2}{\omega^2} \varepsilon\left(\frac{\lambda^2}{2}\right)\right] \frac{\partial E_x}{\partial x}, \tag{11}$$

$$\varepsilon' = 1 - \frac{\omega_p^2}{\omega^2-\omega_c^2 + \dfrac{\omega_p^2\lambda^2}{c^2}\left(1 - \dfrac{\omega_p^2}{c^2k_z^2}\dfrac{\omega^2}{\omega_c^2}\right)\omega^2} + \frac{k_D^2\lambda^2/2}{1 - \dfrac{\omega^2}{c^2k_z^2}\dfrac{k_D^2\lambda^2}{2}}. \tag{12}$$

Contrary to type 3, $E_x(x)$ or $E_y(x)$ is an odd function of x for this coil, so that their x-derivatives are given. We can estimate the value at $x \approx \pm \lambda$, as $E_x \sim \pm \lambda \frac{\partial E_x}{\partial x}$. The B_z° is the rf magnetic field induced by the sheet current I_0. The Eq.(9) shows clearly the screening of the rf field in the plasma just like the parallel electrodes. There is no essential difference in principle between the type 1 and 2. We only have to substitute $I_0/2N$ for type 1, N being the number of turns, to explain the difference of the experimental results between type 1 and 2. One may think of the finite parallel rf electric field in type 1 coil but it is easily screened electrostatically by electrons.

IV. CONCLUSION

It was proved experimentally that the magnetic coupling is more attractive than electrostatic one for a high density plasma, for it requires a lower rf voltage to stop the open-end loss. Particularly, we had the rf plugging independent of plasma density with type 3 coil. It was verified that the rf plugging is effective for the plasma densities up to 10^{14} cm^{-3}. The frequency dependence of rf plugging was also obtained experimentally. The frequency which gives maximum plugging was found lower than ion cyclotron frequency. It differs from the result obtained with parallel plate electrodes in a low density plasma. The theory of rf plugging with magnetic coupling was also presented. It offers the interpretation for the experimentally obtained frequency dependence: the maximum plugging is achieved in a high density plasma when an eigenmode of a transverse wave is excited. On the other hand, it is achieved in a low density plasma when the electrostatic wave is excited. The theory also clarifies the mechanism of the density dependence for each coil. Particularly, it was shown that the electric field induced in the direction of the magnetic field is intrinsic for the density independent result of type 3 coil. Finally we suggest that such an rf plugging is also applicable to other magnetic configurations like a point cusp and a minimum-B.

ACKNOWLEDGEMENTS

The authors wish to thank Prof. A. Miyahara for his technological comments and discussions. They are also indebted to Dr. K. Akaishi for useful discussions about the vacuum system of the TPD-III machine and to Y. Kubota for the design and maintenance of the d.c. power supply.

References

1) D. G. Dow and R. G. Knechtli, J. Electron. Control 7 (1959) 316.

2) S. Miyake, T. Sato, K. Takayama, T. Watari, S. Hiroe, T. Watanabe and K. Husimi, J. Phys. Soc. Jpn. 31 (1971) 265.

3) T. Watari, S. Hiroe, T. Sato and S. Ichimaru, Phys. Fluids 17 (1974) 2107.

4) S. Hiroe, S. Hidekuma, T. Watari, T. Shoji, T. Sato and K. Takayama, Nucl. Fusion 15 (1975) 769.

5) S. Hiroe et al., in Proc. of Seventh Conference on Plasma Physics and Controlled Nuclear Fusion Research, (IAEA, Vienna, 1977) Vol.Ⅲ, p.427.

6) M. Inutake, H. Ikezi and K. Kuriki, in Modern Developments in Shock Tube Research (Edited by G. Kamimoto, Shock Tube Research Society, Japan, 1975) p.714.

7) S. S. Ovchinnikov et al., in Proc. of Fourth Conference on Plasma Physics and Controlled Nuclear Fusion Research, (IAEA, Vienna, 1971) Vol.Ⅲ, p.597.

8) T. H. Stix, The Theory of Plasma Waves (McGraw-Hill Book Company, New York, 1962).

Figure Captions

Fig.1 The experimental setup.

Fig.2 The profile of the magnetic field intensity. The rf coil is set up in the shaded region.

Fig.3 Schematic diagram of rf coils.

Fig.4 a) The loss flux when TPD source is used; time scale is 5 ms/div. b) the loss flux when MPD source is used; time scale is 200 μs/div.

Fig.5 The dependence of loss flux on rf voltage.

Fig.6 The rf voltage versus plasma density required to reduce the loss flux to 10%.

Fig.7 The frequency dependence of the rf plugging. A He^+ plasma whose density is 1.5×10^{13} cm^{-3} is used. The magnetic field in the center of the rf coil is 12.2 kG.

Fig.8 The dependence of the optimum frequency for plugging on the rf voltage.

Fig.9 The coordinate systems. a) model for the parallel plate rf electrode. b) model for the type 2 coil. c) model for the type 3 coil. The vacuum electromagnetic rf fields are shown.

Fig.10 The contour which gives $\varepsilon = 0$. We gave $(\omega_p^2/\omega_c^2) = 7600$, $(T_i\lambda^2/T_e\rho_i^2) = (\lambda^2 m\omega_c^2/T_e) = 275$, and $(c^2/\omega_p^2\lambda^2) = 139$ in the calculation corresponding to the experimental condition $B = 12.2$ kG, $T_e = 13$ eV, $T_i = 15$ eV, and $n = 1.5 \times 10^{13}$ cm^{-3}. The arrow in the figure indicates the experimental condition which gives Fig.7.

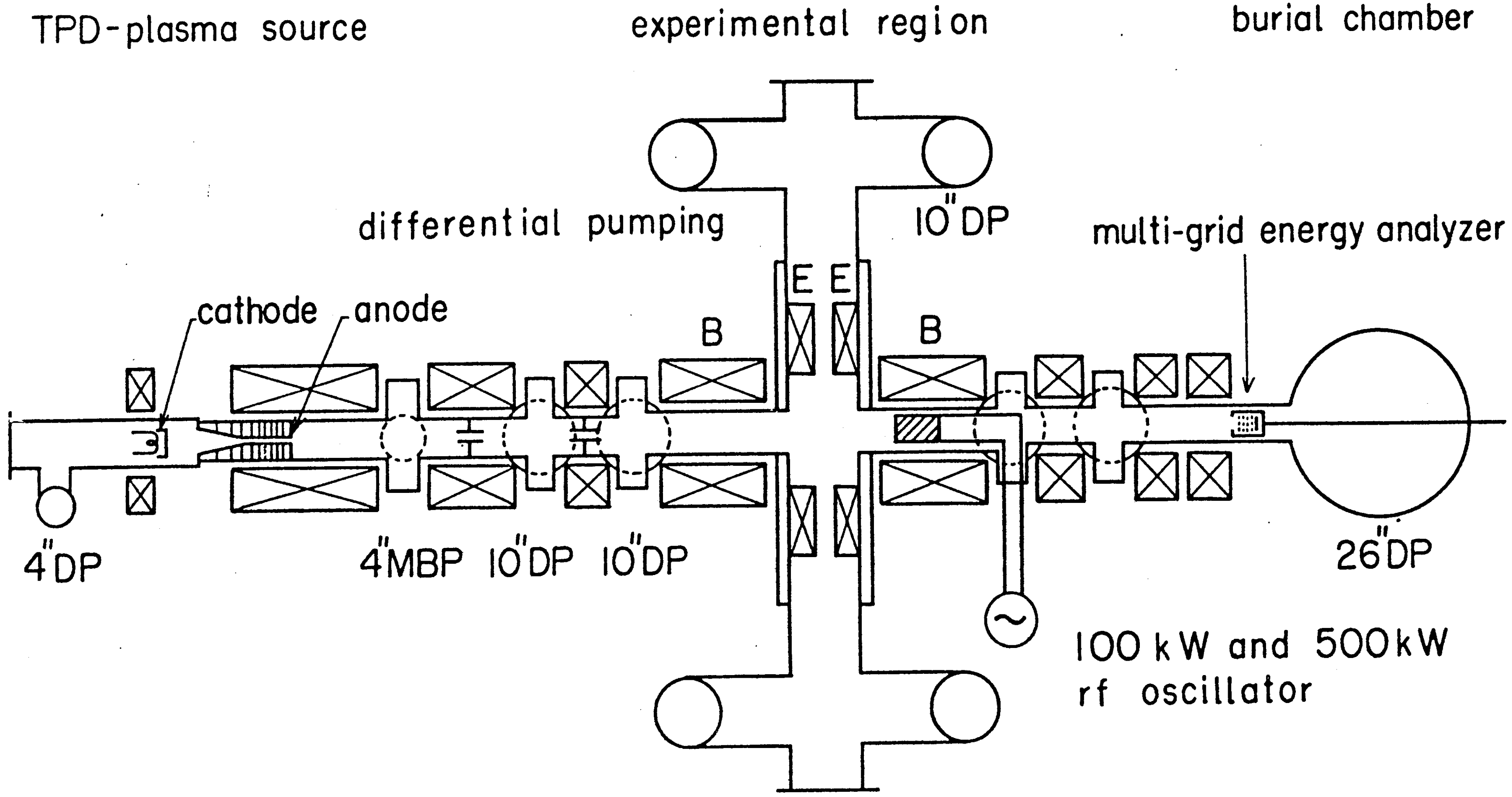
TPD-plasma source
experimental region
burial chamber
differential pumping
10" DP
multi-grid energy analyzer
cathode
anode
B
E
E
B
4" DP
4" MBP
10" DP
10" DP
26" DP
100 kW and 500 kW
rf oscillator

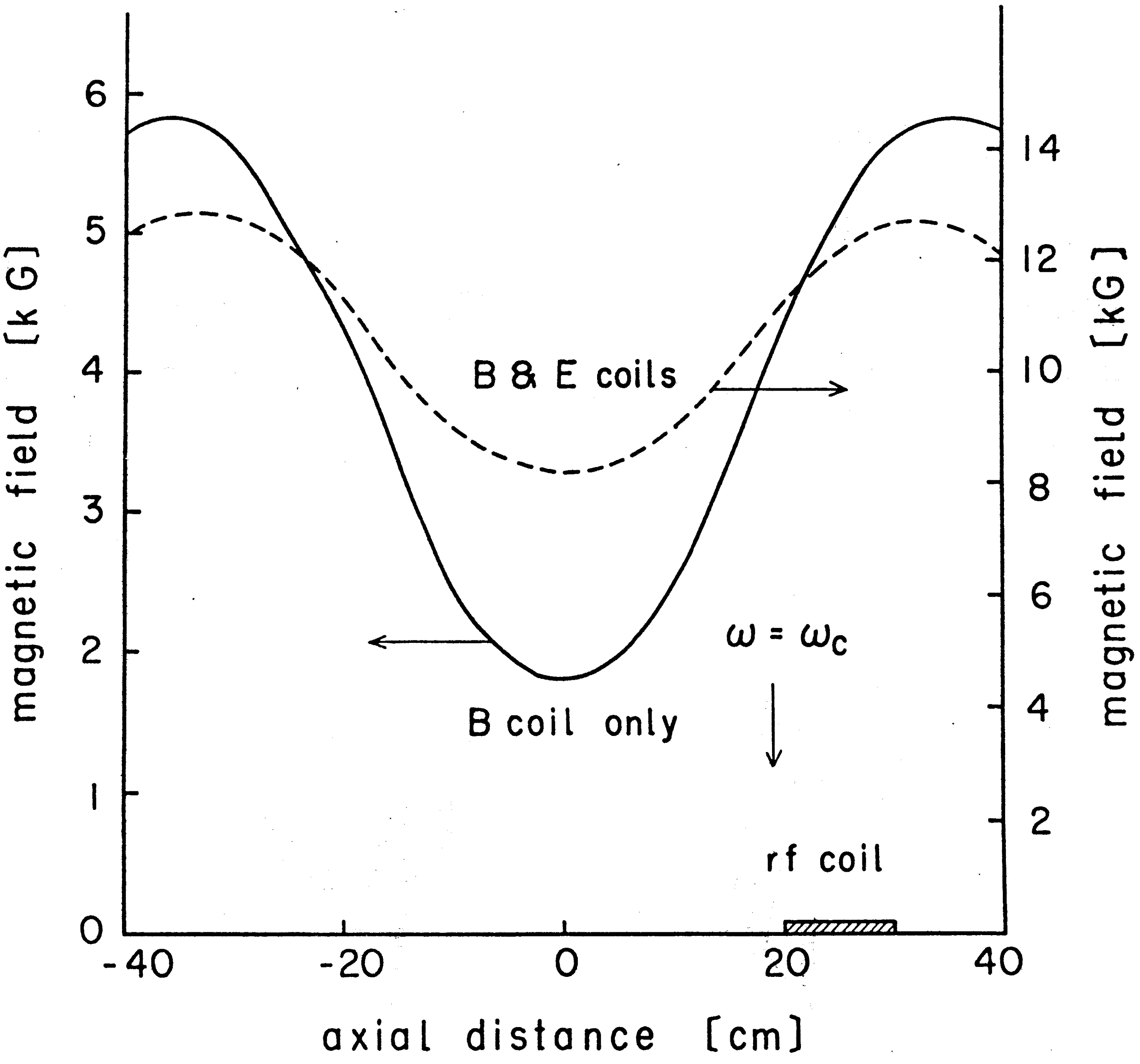
magnetic field [k G]
0
1
2
3
4
5
6
magnetic field [kG]
2
4
6
8
10
12
14
B & E coils
B coil only
$\omega = \omega_c$
rf coil
-40
-20
0
20
40
axial distance [cm]

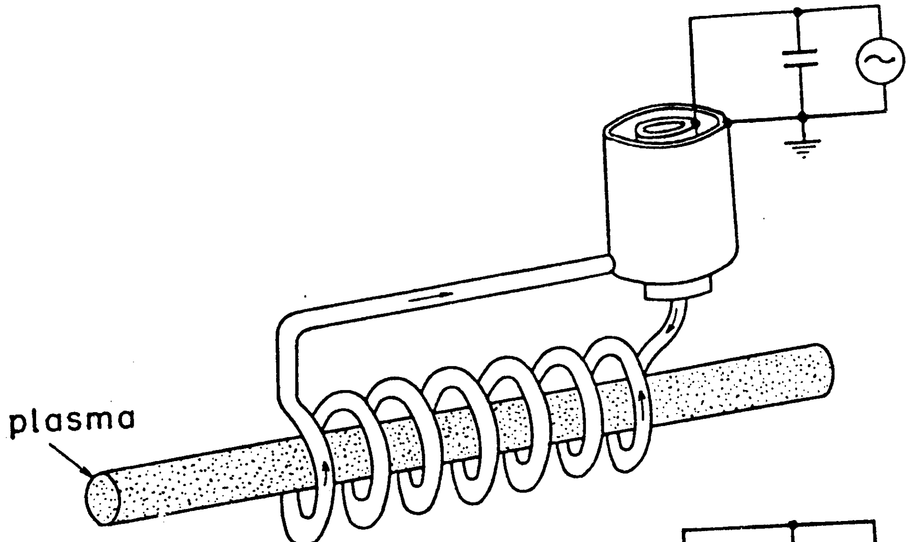

Type 1 coil

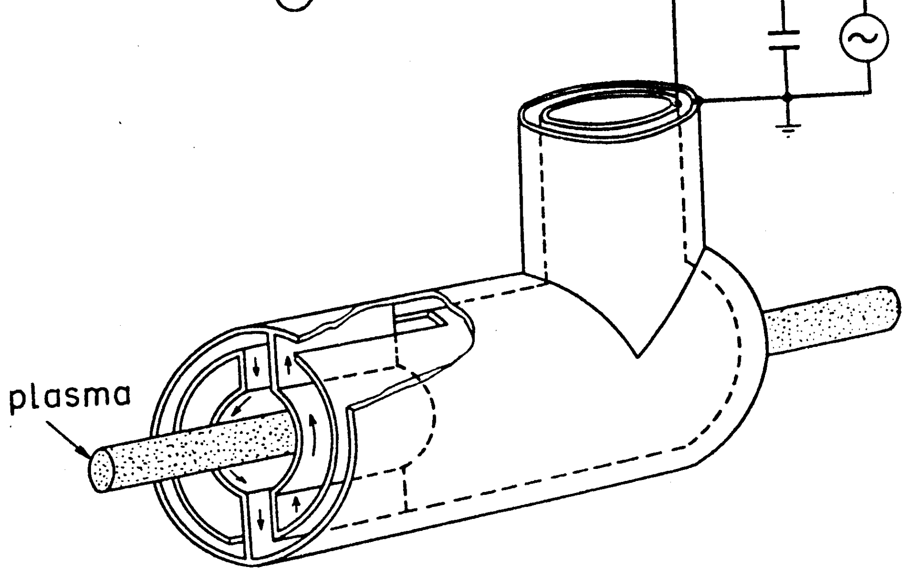

Type 2 coil

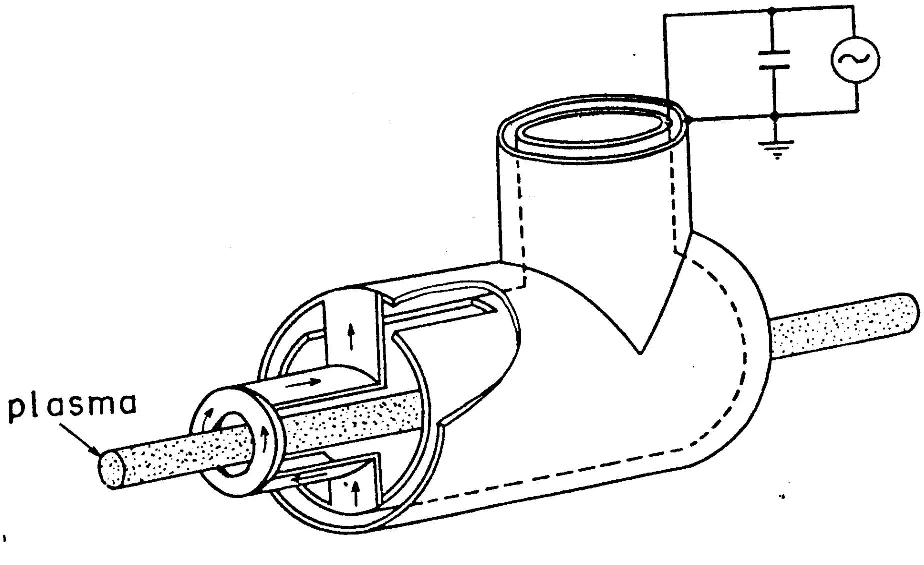

Type 3 coil

a)

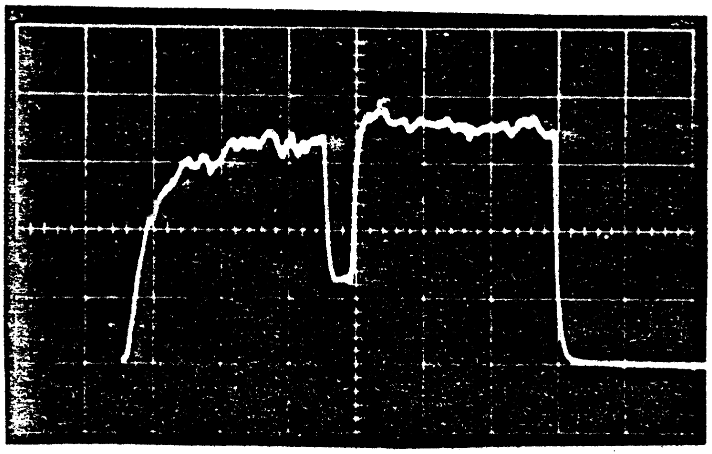

b)

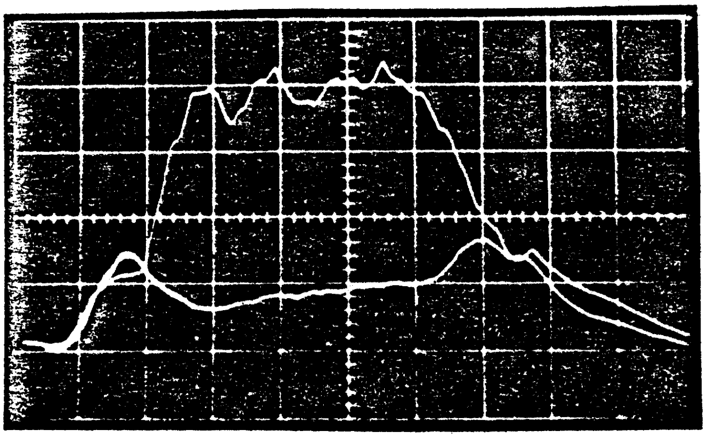

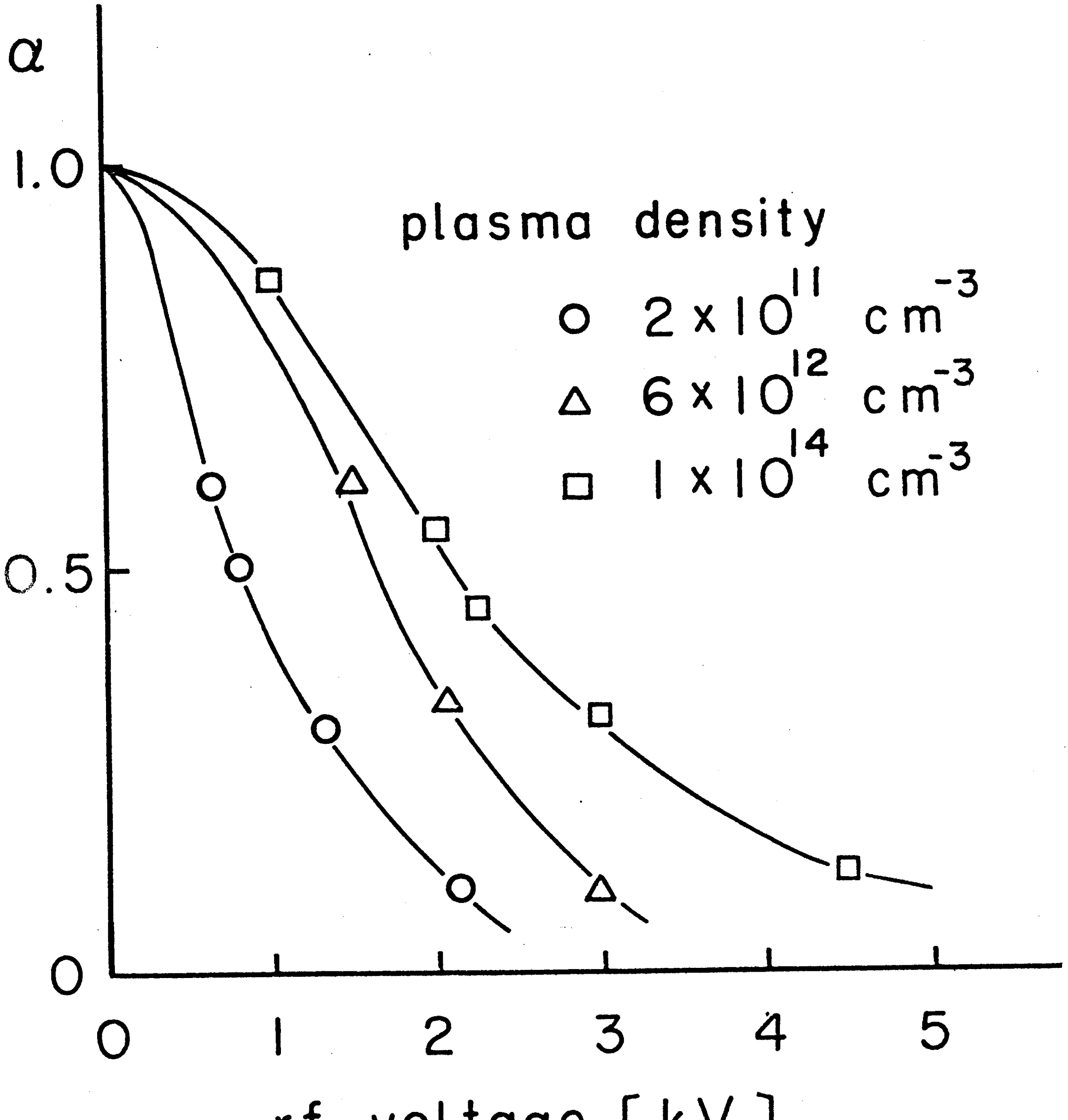
α
1.0
0.5
0
plasma density
○ 2 x 10^11 cm^-3
△ 6 x 10^12 cm^-3
□ 1 x 10^14 cm^-3
0
1
2
3
4
5
rf voltage [kV]

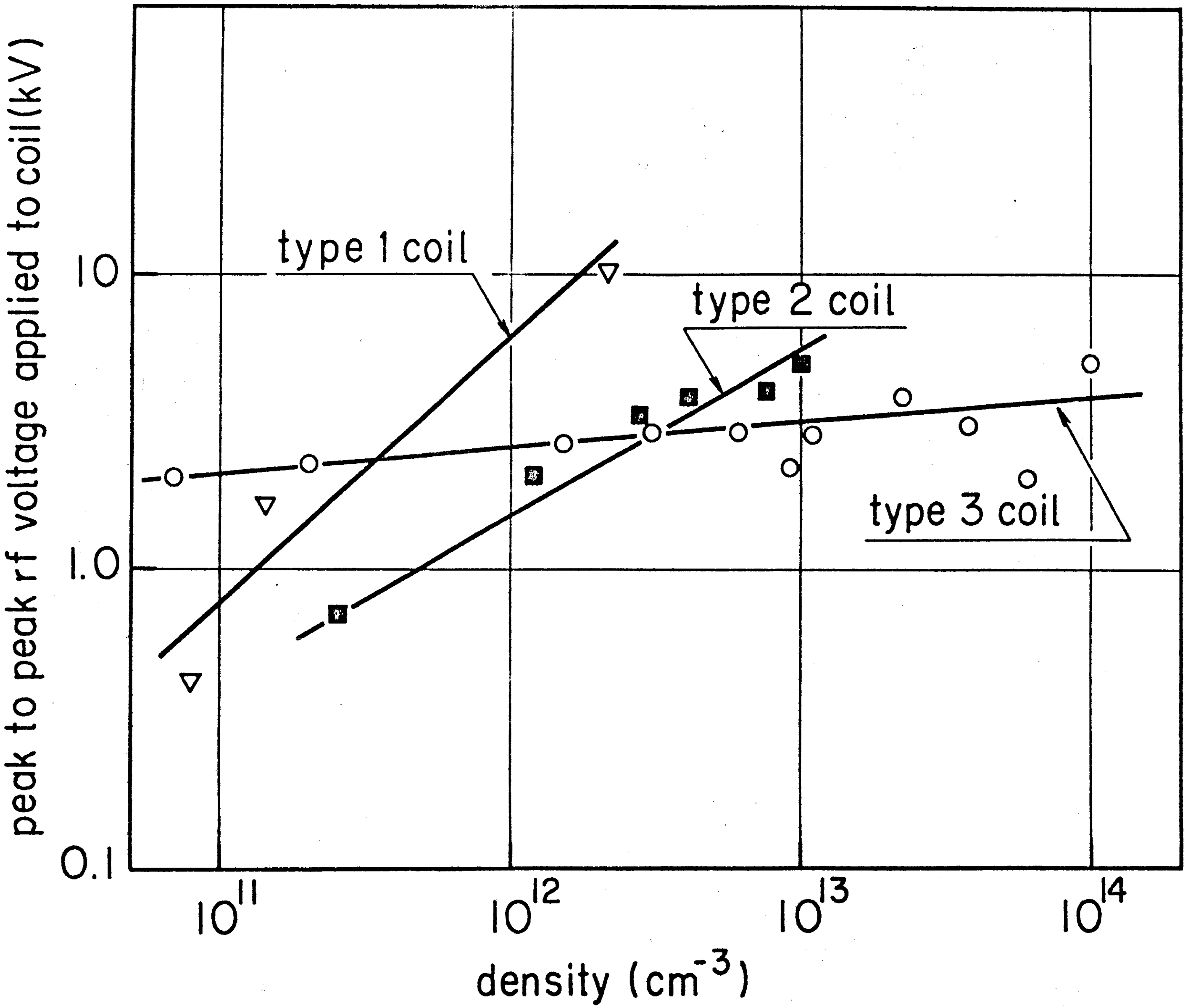
type 1 coil
type 2 coil
type 3 coil
peak to peak rf voltage applied to coil(kV)
10
1.0
0.1
10^{11}
10^{12}
10^{13}
10^{14}
density (cm^{-3})

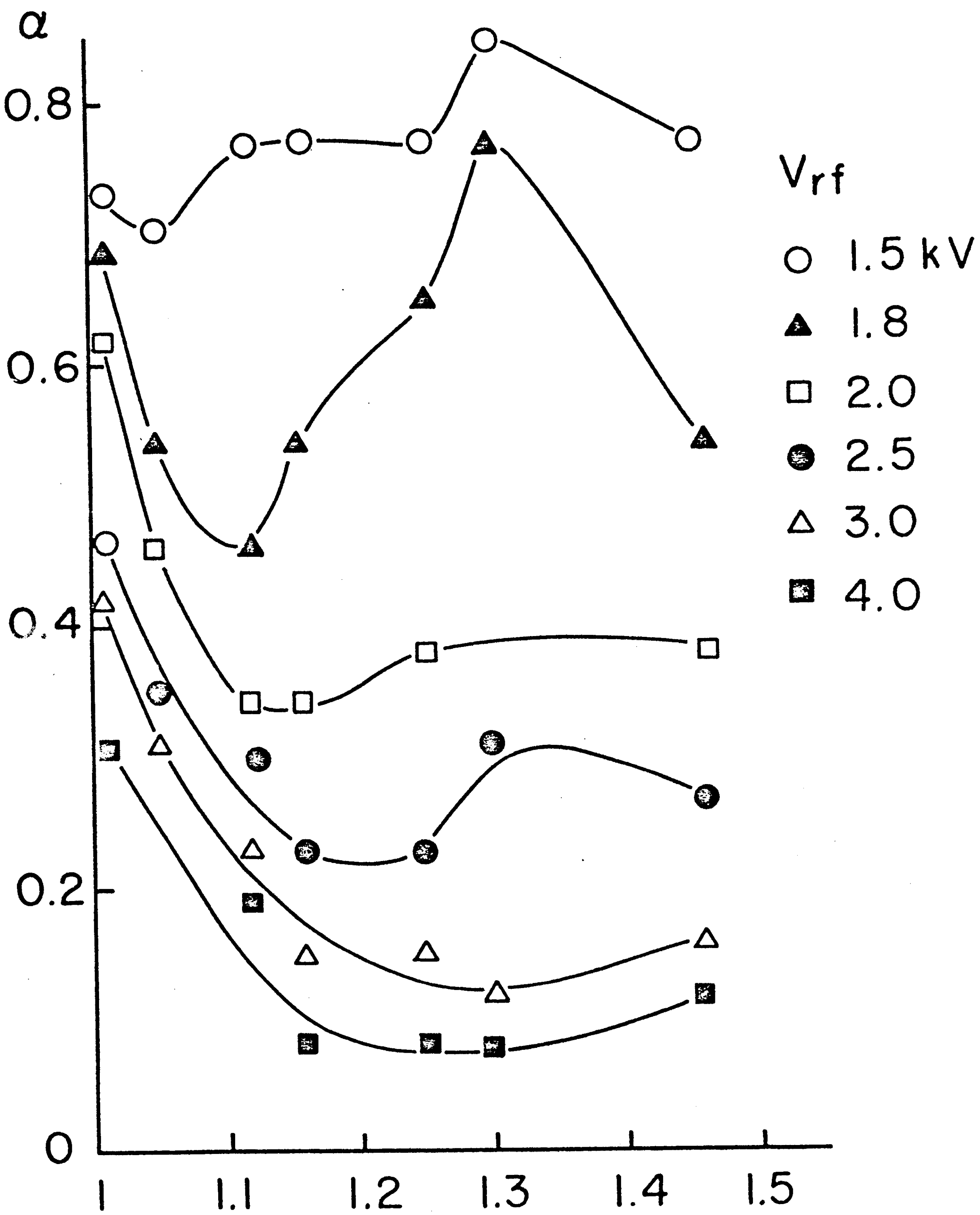
α
0.8
0.6
0.4
0.2
0
1
1.1
1.2
1.3
1.4
1.5
ω / ω_c
V_rf
○ 1.5 kV
▲ 1.8
□ 2.0
● 2.5
△ 3.0
■ 4.0

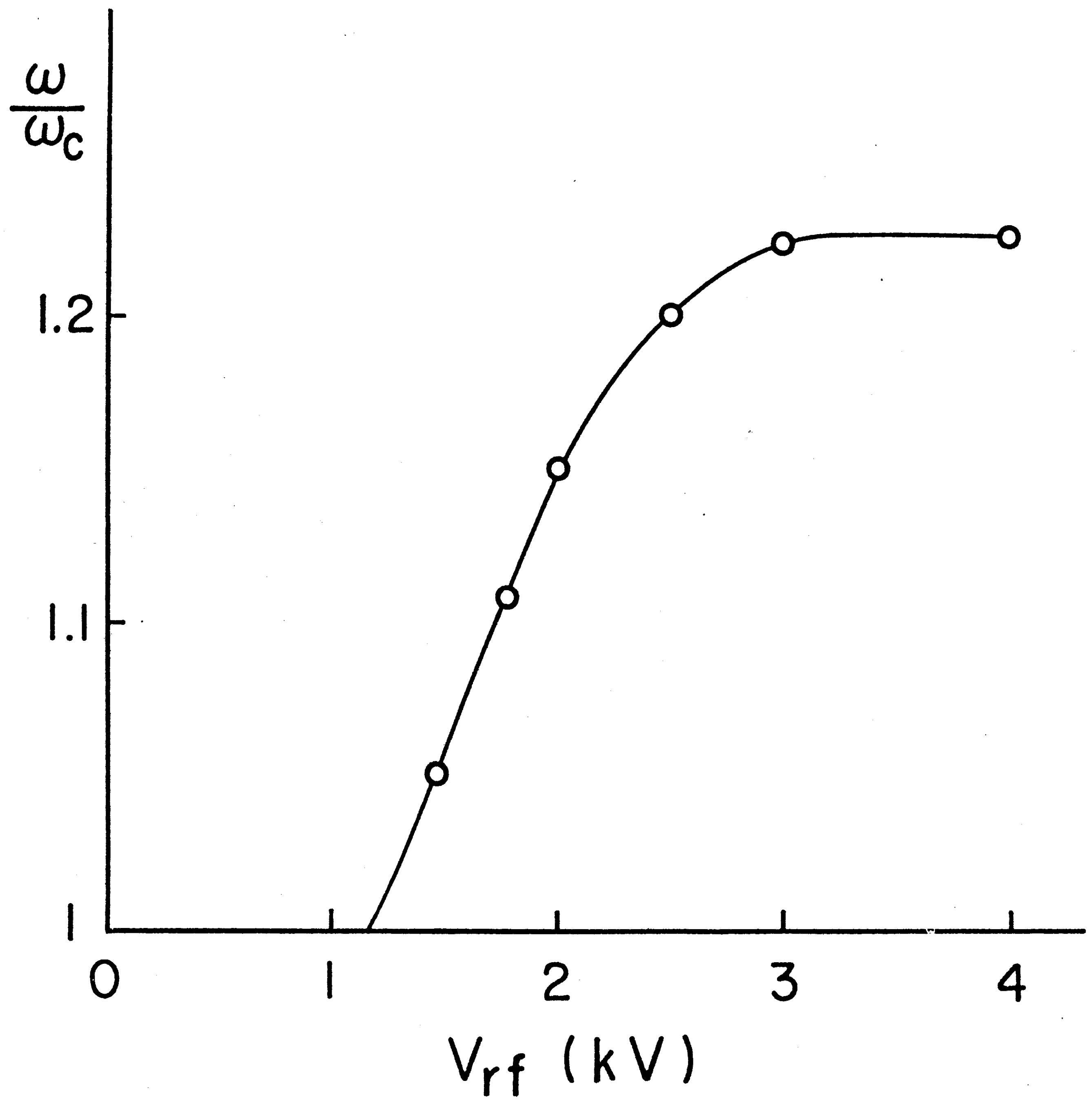
$\frac{\omega}{\omega_c}$
1.2
1.1
1
0
1
2
3
4
V_{rf} (kV)

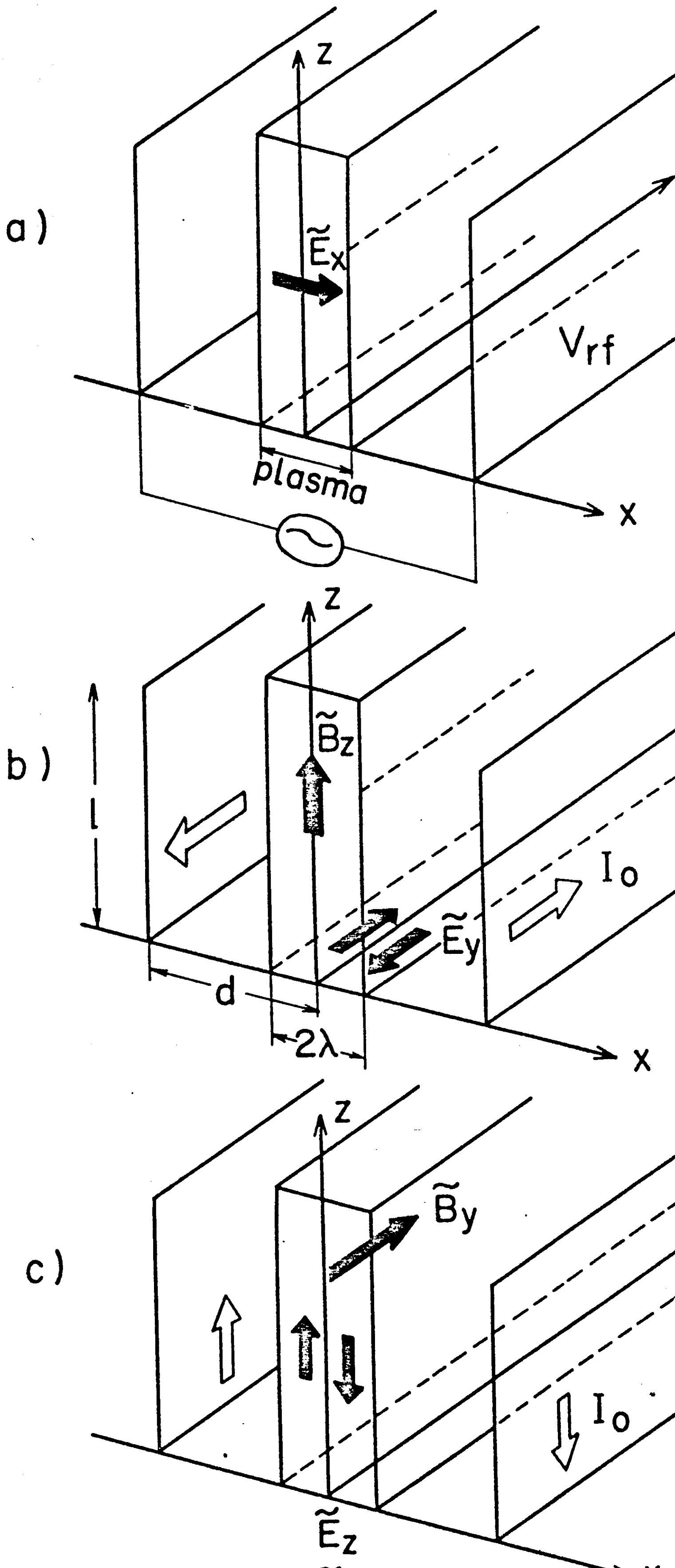
a)
z
y
$\tilde{E}_x$
V_{rf}
plasma
x
b)
z
y
$\tilde{B}_z$
l
I_o
$\tilde{E}_y$
d
2λ
x
c)
z
$\tilde{B}_y$
y
I_o
$\tilde{E}_z$
$\tilde{I}_z$
x

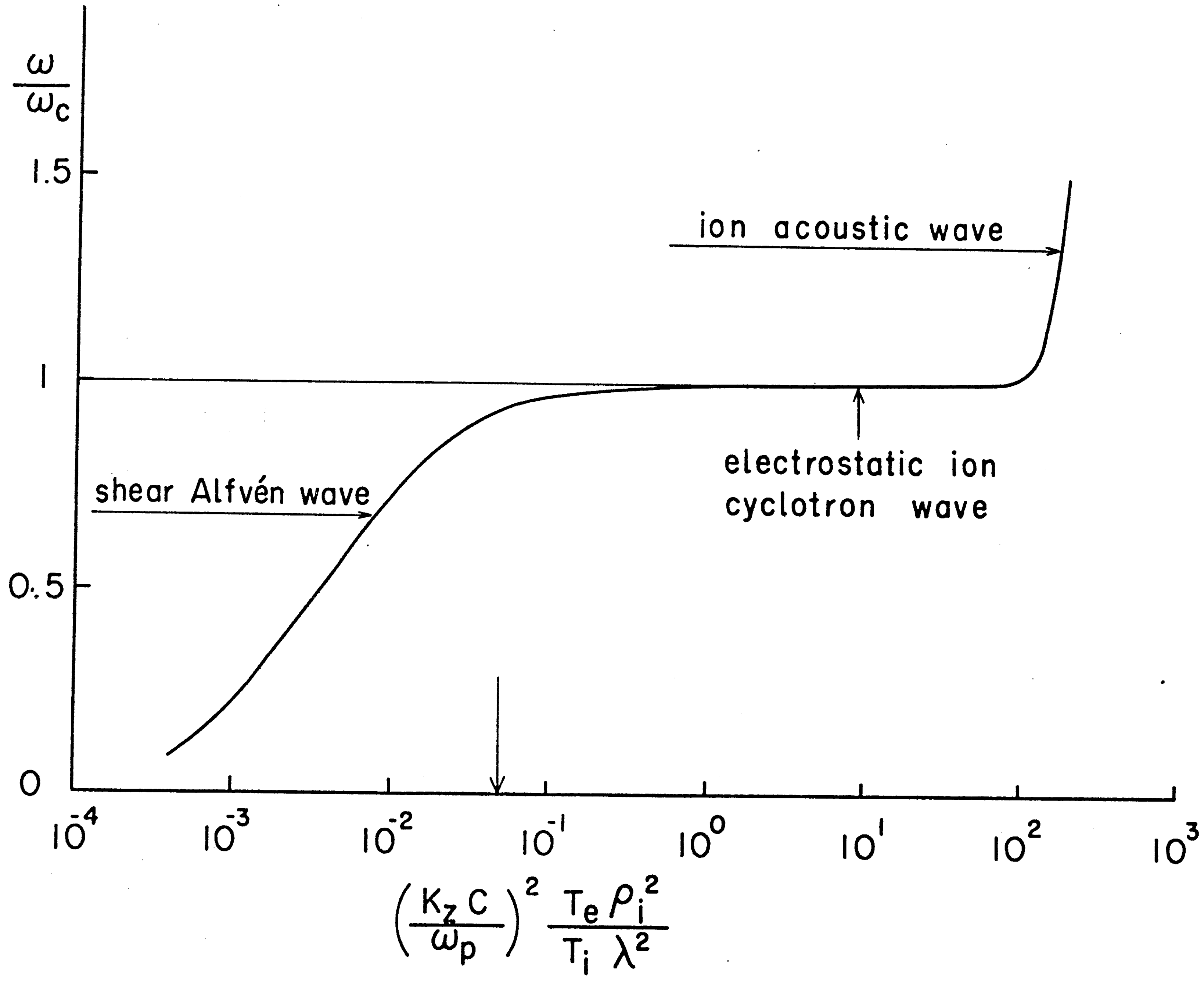
$\frac{\omega}{\omega_c}$
1.5
1
0.5
0
10^{-4}
10^{-3}
10^{-2}
10^{-1}
10^{0}
10^{1}
10^{2}
10^{3}
$\left(\frac{K_z C}{\omega_p}\right)^2 \frac{T_e \rho_i^2}{T_i \lambda^2}$
ion acoustic wave
shear Alfvén wave
electrostatic ion
cyclotron wave